

Template-Assisted Three-Dimensional Nanolithography via Geometrically Irreversible Processing

Xindi Yu,[†] Huigang Zhang,[†] John K. Oliverio, and Paul V. Braun^{*}

Department of Materials Science and Engineering, Frederick Seitz Materials Research Laboratory and Beckman Institute, University of Illinois at Urbana-Champaign, Urbana, Illinois 61801

Received August 20, 2009; Revised Manuscript Received October 29, 2009

ABSTRACT

An innovative and versatile nanofabrication technique based on template assisted three-dimensional (3D) nanolithography is presented that takes advantage of the irreversibility of conformal growth and conformal etching at locations with negative surface curvatures in 3D templates. Using colloidal crystals as templates, nanoring particles are generated with quantity much higher than conventional methods. Relying on the same principle, metallocodielectric photonic crystals with discrete metal elements are fabricated that show strong absorption in the near-IR and transmission at longer wavelengths.

In recent years, considerable efforts have been put into combining conventional top-down nanofabrication and self-assembly based bottom-up methods to generate a diversity of complex nanostructures.^{1–3} For example, through nanosphere lithography, a process that uses a colloidal monolayer as a deposition or etch mask, a variety of innovative two-dimensional (2D) nanostructures including triangles, rings, dots, and honeycomb structures have been generated.⁴ However, the resulting patterns are generally limited to two-dimensional structures of certain specific symmetries. Here we present a three-dimensional (3D) template-assisted nanofabrication technique that uniformly generates metallic and ceramic nanostructures throughout self-assembled colloidal templates. This method allows us to position the nanostructured objects at specific locations within the template, forming highly periodic multicomponent composite structures. Dissolving the template releases large quantities of unique shaped particles. Because the nanostructures are produced throughout the 3D template, much higher quantities of particles are generated than for a 2D fabrication process. In particular, ring-shaped particles have attracted considerable attention because of their unique plasmonic,⁵ optical,⁶ and magnetic properties⁷ depending on the choice of materials. Two-dimensional based colloidal lithography has been a very popular method to generate particles of this kind.⁴ However, each colloid in the colloidal monolayer only generates one ring particle, greatly limiting the quantities of particles

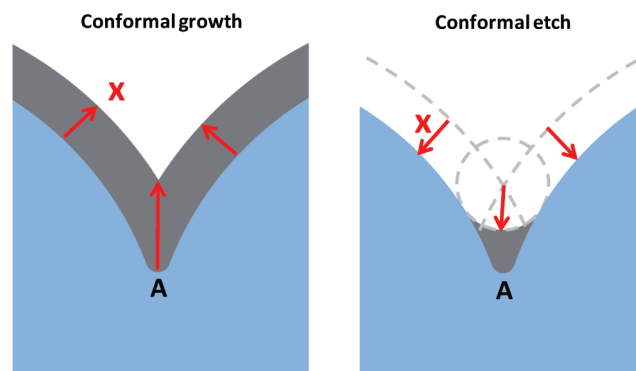


Figure 1. Schematic of an irreversible conformal growth (left) and conformal etching (right) process in two dimensions. After deposition and etching of the same thickness of material, some material remains in areas with a small negative radius of curvature.

generated per unit area. The advantages of a 3D lithographic approach are obvious, since all the colloids in the 3D colloidal crystal are utilized and each colloid generates 6 ring particles. As a result, particle areal density is increased by 2 orders of magnitude over a monolayer process.

The method proposed here takes advantage of the fact that conformal etching is not the geometric reverse of conformal growth at locations with negative surface curvature. A simple 2D representation illustrating this is shown in Figure 1. When the conformal coating thickness exceeds the minimum radius of the negative curvature, shown at point A in Figure 1, the growth front along the normal direction moves faster than the rate of conformal coating. However, conformal etching propagates at the same rate along all directions. As a result,

* To whom correspondence should be addressed. E-mail: pbraun@illinois.edu.

[†] These authors contributed equally.

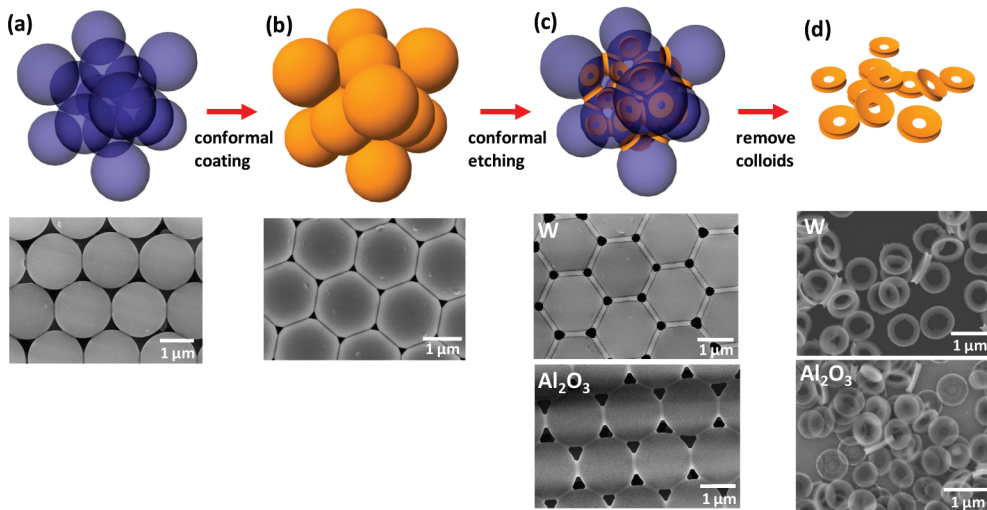


Figure 2. Schematic diagram and SEM images of the four stages of the process for synthesizing ring particles. (a) Colloidal crystal template formed by self-assembly, SEM image shows a crystalline silica colloidal film; (b) after conformal coating by CVD or ALD, SEM shows a tungsten CVD coated silica colloidal crystal; (c) ring particles formed in between colloids after conformal wet etch, SEM images show tungsten and Al_2O_3 ring particles formed at the silica and polystyrene colloid contact points, respectively; (d) released ring particles, SEM images show well-dispersed tungsten and Al_2O_3 ring particles after etching of the colloidal crystal template.

when the etching thickness equals the coating thickness, some coating material is left in the area originally having negative surface curvature.

Three-dimensional colloidal crystals composed of close-packed silica or polymer spheres are good examples of structures abundant of negative curvatures at the contact point of each pair of spheres. Using these as templates, nanoring particles can be fabricated as illustrated in Figure 2. First a smooth film of tungsten with uniform thickness is coated onto a 3D silica colloid template through a static chemical vapor deposition (CVD) process (Figure 2b).⁸ Then, the tungsten-coated sample is anodized in a sulfuric acid solution, converting roughly 10 nm of the surface of the tungsten to tungsten oxide.⁹ The oxide layer is etched away in a potassium hydroxide solution. This process of anodization followed by chemical etching is repeated multiple times until the tungsten coated on the surface of the spheres other than the contact region is completely etched away, resulting in tungsten rings at the contact points between spheres (Figure 2c). It is worthwhile to point out that for this specific system, the tungsten coating layer functions as the conductive pathway in the anodization step. Once a tungsten ring is electrically disconnected from the substrate, it is no longer etched. This makes the anodization a self-limiting process. As a result, even if the anodization is not completely uniform through the thickness of the template, the resulting tungsten rings are still quite monodispersed. After etching of the colloids in a dilute hydrofluoric acid (HF) solution followed by a washing and centrifugation step, the tungsten nanoring particles can be harvested (Figure 2d). A distinct advantage of this nanoring fabrication process is that it does not require a perfect colloidal crystal template, since the rings are only formed at each colloid pair contact point. So, even a randomly packed colloidal film can be used (Supporting Information Figure S1). Electron diffraction (Supporting Information Figure S2) indicates the rings are amorphous as expected for the CVD process utilized. The same principle

can be applied to any material as long as the conformal coating and etching process exist, which are compatible with the template being used. Aluminum oxide rings are generated by coating polystyrene colloidal crystal with Al_2O_3 through atomic layer deposition (ALD) followed by a slow HF etching (bottom SEM images of Figure 2c,d) (details in Supporting Information).

The dimension of the rings generated can be easily calculated by simple geometry. R is the radius of the colloidal spheres; x is the thickness of the conformal coating layer and also the conformal etching layer (assuming they are equal); r and h are the radius and thickness of the ring particle.

$$r = \sqrt{x^2 + 2xR} - x \sim \sqrt{2xR} - x$$

$$h = \frac{2xR}{x + R} \sim 2x$$

The approximation is valid when $x \ll R$ (in real case, x/R is <0.15 due to geometrical constraints). Since both x and R can be independently selected, the radius and the thickness of the ring particles can be independently controlled as shown in the Figure 3a,b, where tungsten films of two different thickness, 60 and 40 nm, respectively, are coated on colloidal template grown using 1.58 μm diameter colloids. The thicker coating generates rings of greater thickness, 132 nm versus 93 nm, and diameter, 640 nm versus 454 nm. When colloidal templates of different sizes, 1.58 μm versus 920 nm, are coated with tungsten with the same thickness (40 nm), the radii of the final ring particles vary, 454 nm versus 328 nm, while the thicknesses are kept roughly the same, 93 nm versus 89 nm (Figure 3b,c). By scaling the colloid size and coating thickness together, ring particles of different sizes but similar in aspect ratio are generated (Figure 3a,d). Detailed dimensions of tungsten particle in each case are listed in Table 1. SEM images of released ring particles fabricated from templates of different colloid sizes are shown in Supporting Information Figure S4. The ability to inde-

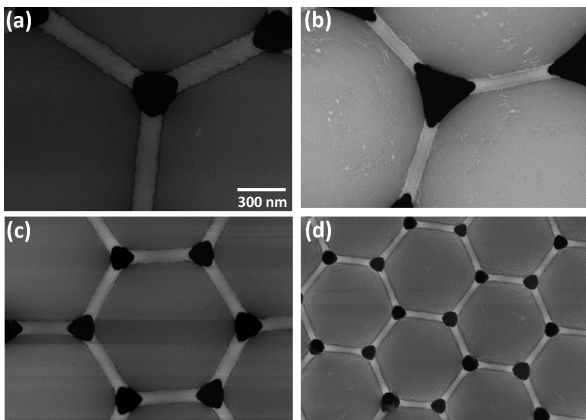


Figure 3. (a–d) SEM images of tungsten ring particles before release from the colloidal template. All images are of the same magnification. The diameter and the thickness of the rings can be independently adjusted by using colloids of different sizes as templates and by varying the conformal coating thickness (see Table 1 for numerical values).

Table 1. Geometric Parameters of Colloidal Templates and Ring Particles Presented in Figure 3

colloid diameter (nm)	W coating thickness (nm)	ring particle diameter (nm) \pm standard deviation (nm)	ring particle thickness (nm) \pm standard deviation (nm)
(a)	1580	60	640 ± 58
(b)	1580	40	454 ± 93
(c)	920	40	328 ± 37
(d)	550	20	220 ± 12

pendently modulate the dimensions of the resulting nanoparticles could be advantageous for numerous applications.

Along with providing a relatively high volume nanostructure fabrication process, this 3D lithography method results in a unique metallocodielectric photonic crystal consisting of disconnected metallic elements supported by a dielectric structure. Popular methods for generating 3D metallocodielectric photonic crystal involve the use of templates formed by colloidal self-assembly,¹⁰ interference lithography^{11,12} or direct writing^{13,14} which are filled with a metal by conformal coating,¹⁵ nanoparticle infilling,^{16,17} or electrodeposition.¹⁸ The result is a connected metallic structure in which electric fields are conductively coupled. Three-dimensional optical metamaterials based on resonant structures require discrete capacitively coupled metal elements to be positioned inside a 3D matrix with accurate control over their position, geometry, and orientation.^{19,20} In those cases, conductive coupling of the metallic elements is undesirable. The ability to position disconnected metallic elements in 3D space using a colloidal crystal template and our template assisted three-dimensional nanolithography process is demonstrated for the case of tungsten rings generated in a 3D silica colloidal crystal (Figure 4a). Here, the disconnected tungsten rings form a periodic structure corresponding to Wyckoff notation 24d of space group $Fm\bar{3}m$ with the ring axis normal to the colloid surface. The reflection and transmission spectra of the template (Figure 4b) and the metallocodielectric photonic crystal after all processing steps (Figure 4c) are measured. Strong absorption is observed around $2.5 \mu\text{m}$, while a pass band at long wavelengths is indicative of the discrete nature

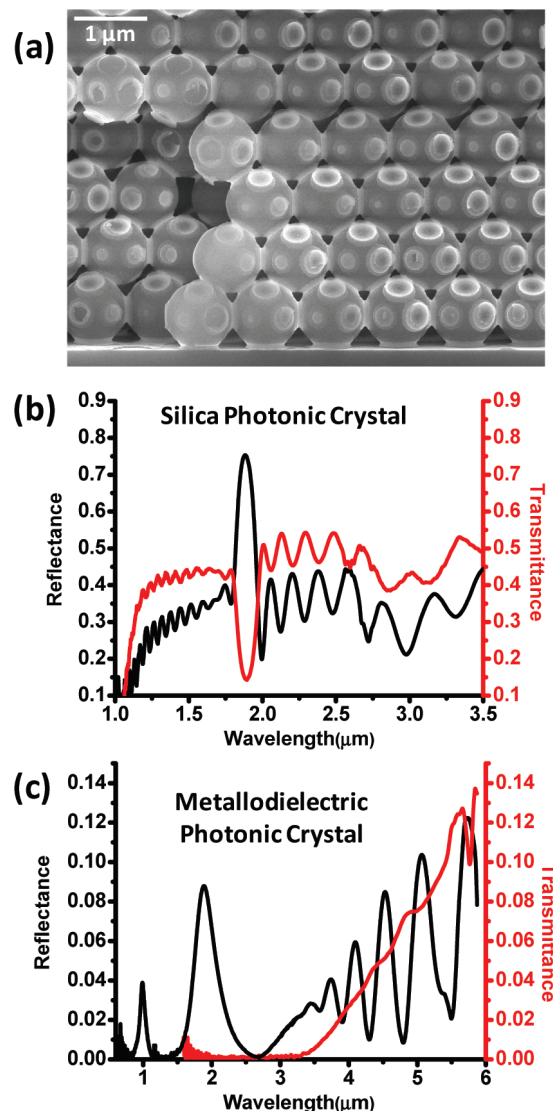


Figure 4. Metallocodielectric photonic crystal composed of discrete W ring particles formed *in situ* using a 920 nm diameter silica colloidal crystal template. (a) Cross-section SEM image of the metallocodielectric colloidal crystal. Discrete tungsten ring particles are clearly seen. (b) Reflection (black trace) and transmission (red trace) spectra of silica colloidal crystal template before tungsten deposition. (c) Reflection (black trace) and transmission (red trace) spectra of metallocodielectric photonic crystal shown in (a) after W deposition and etching.

of the metal elements. Although the structure shown here is not a metamaterial, which requires resonance elements such as split rings²¹ and a lower loss metal than CVD tungsten, we believe that by designing and fabricating a proper template with the appropriate curvature distribution using methods such as interference lithography or direct writing^{11–14} and by choosing the right low loss materials, such structures may be achievable.

In summary, we describe an innovative fabrication technique, template-assisted 3D nanolithography. Using colloidal crystals as templates, nanoring particles and metallocodielectric photonic crystals are fabricated. The combination of this approach with more complex templates with designed negative curvature distribution, for example, those formed through optical interference,^{11,22–24} may provide a path to

otherwise unobtainable nanostructures and complex photonic structures.

Acknowledgment. The authors thank Erik Nelson for helpful discussions and for providing some materials used in this work, Dr. Jianguo Wen (CMM) for assistance in TEM characterization, and Professor Dallas Trinkle for valuable discussions regarding crystallography. This material is based on work supported by the U.S. Department of Energy, Division of Materials Sciences under Award No. DE-FG02-07ER46471, through the Frederick Seitz Materials Research Laboratory at the University of Illinois at Urbana-Champaign.

Supporting Information Available: Tungsten rings formed in random colloidal film, TEM images, and electron diffraction pattern from an individual W ring particle, SEM image of large quantities of tungsten rings solvent cast on a Si wafer, reflection, and transmission spectra of metallocodielectric photonic crystals as a function of number of layers, reflection, and transmission spectrum of refractive index matched dielectric template and metallocodielectric photonic crystal, and experimental details. This material is available free of charge via the Internet at <http://pubs.acs.org>.

References

- (1) Hawker, C. J.; Russell, T. P. *MRS Bull.* **2005**, *30*, 952–966.
- (2) Chik, H.; Xu, J. M. *Mater. Sci. Eng. R* **2004**, *43*, 103–138.
- (3) Li, Y.; Cai, W.; Duan, G. *Chem. Mater.* **2008**, *20*, 615–624.
- (4) Yang, S. M.; Jang, S. G.; Choi, D. G.; Kim, S.; Yu, H. K. *Small* **2006**, *2*, 458–475.
- (5) Anker, J. N.; Hall, W. P.; Lyandres, O.; Shah, N. C.; Zhao, J.; Van Duyne, R. P. *Nat. Mater.* **2008**, *7*, 442–453.

- (6) Little, B. E.; Foresi, J. S.; Steinmeyer, G.; Thoen, E. R.; Chu, S. T.; Haus, H. A.; Ippen, E. P.; Kimerling, L. C.; Greene, W. *IEEE Photonics Technol. Lett.* **1998**, *10*, 549–551.
- (7) Zhu, F. Q.; Fan, D. L.; Zhu, X. C.; Zhu, J. G.; Cammarata, R. C.; Chien, C. L. *Adv. Mater.* **2004**, *16*, 2155.
- (8) Nagpal, P.; Han, S. E.; Stein, A.; Norris, D. J. *Nano Lett.* **2008**, *8*, 3238–3243.
- (9) Anik, M.; Osseo-Asare, K. *J. Electrochem. Soc.* **2002**, *149*, B224–B233.
- (10) Wong, S.; Kitaev, V.; Ozin, G. A. *J. Am. Chem. Soc.* **2003**, *125*, 15589–15598.
- (11) Campbell, M.; Sharp, D. N.; Harrison, M. T.; Denning, R. G.; Turberfield, A. J. *Nature* **2000**, *404*, 53–56.
- (12) Jeon, S.; Park, J. U.; Cirelli, R.; Yang, S.; Heitzman, C. E.; Braun, P. V.; Kenis, P. J. A.; Rogers, J. A. *Proc. Natl. Acad. Sci. U.S.A.* **2004**, *101*, 12428–12433.
- (13) Deubel, M.; Von Freymann, G.; Wegener, M.; Pereira, S.; Busch, K.; Soukoulis, C. M. *Nat. Mater.* **2004**, *3*, 444–447.
- (14) Gratson, G. M.; Xu, M. J.; Lewis, J. A. *Nature* **2004**, *428*, 386–386.
- (15) Rill, M. S.; Plet, C.; Thiel, M.; Staude, I.; Von Freymann, G.; Linden, S.; Wegener, M. *Nat. Mater.* **2008**, *7*, 543–546.
- (16) Chen, H. H.; Suzuki, H.; Sato, O.; Gu, Z. Z. *Appl. Phys. A* **2005**, *81*, 1127–1130.
- (17) Liang, Z. J.; Susha, A. S.; Caruso, F. *Adv. Mater.* **2002**, *14*, 1160–1164.
- (18) Bartlett, P. N.; Ghanem, M. A.; El Hallag, I. S.; de Groot, P.; Zhukov, A. J. *Mater. Chem.* **2003**, *13*, 2596–2602.
- (19) Pendry, J. B.; Holden, A. J.; Robbins, D. J.; Stewart, W. J. *IEEE Trans. Microwave Theory Tech.* **1999**, *47*, 2075–2084.
- (20) Koschny, T.; Zhang, L.; Soukoulis, C. M. *Phys. Rev. B* **2005**, *71*, 121103.
- (21) Linden, S.; Enkrich, C.; Wegener, M.; Zhou, J. F.; Koschny, T.; Soukoulis, C. M. *Science* **2004**, *306*, 1351–1353.
- (22) Chen, Y. C.; Geddes, J. B.; Lee, J. T.; Braun, P. V.; Wiltzius, P. *Appl. Phys. Lett.* **2007**, *91*, 241103.
- (23) Pang, Y. K.; Lee, J. C. W.; Lee, H. F.; Tam, W. Y.; Chan, C. T.; Sheng, P. *Opt. Express* **2005**, *13*, 7615–7620.
- (24) Rinne, J. W.; Wiltzius, P. *Opt. Express* **2006**, *14*, 9909–9916.

NL9027236